Hardness and fracture toughness of brittle materials: A density functional theory study

Zenong Ding,[1] Shujia Zhou,[2,*] and Yusheng Zhao[3]
[1]*Department of Chemistry, Northwestern University, Evanston, Illinois 60208, USA*
[2]*Department of Mechanical Engineering, The Johns Hopkins University, Baltimore, Maryland 21218, USA*
[3]*Los Alamos National Laboratory, Los Alamos, New Mexico 87545, USA*
(Received 22 December 2003; revised manuscript received 28 May 2004; published 18 November 2004)

The focus of the paper is to study the correlation between hardness and fracture toughness of brittle materials. To this end, density functional theory (DFT) is used to calculate materials parameters such as the surface energies, the unstable stacking fault energies, the Young's modulus, the bulk modulus, the shear moduli, and the Poisson's ratio of crystalline B_6O as well as the surface energies of *c*BN and 3C—SiC. With these calculated materials parameters as well as reported ones, the theoretical fracture toughness of diamond, *c*BN, B_6O, 3C—SiC, and Si are obtained and compared with experimental hardness. We find that the theoretical fracture toughness, proportional to the product of shear modulus and surface energy, can better characterize hardness of diamond, *c*BN, B_6O, 3C—SiC, Si, and possibly other brittle materials than shear modulus alone [D. M. Teter, MRS Bull. **23**, 22 (1998)]. This finding could be helpful in searching for new hard materials.

DOI: 10.1103/PhysRevB.70.184117 PACS number(s): 62.20.Mk, 62.20.Qp, 62.20.Dc

I. INTRODUCTION

Even though experimental methods to measure hardness such as Vickers, Snoop, etc.[1] have been used for decades, a theory relating materials physics to hardness measurements has not been well developed simply because the physical process occurring in hardness measurements is very complex, involving fracture and deformation under mixed loading conditions (see Zhang and Subhas[2]). However, there do exist several observations which attempt to establish correlation between hardness and one single elastic property such as bulk modulus[3–5] or shear modulus.[6,7] After comparing the measured values of hardness in a set of hard materials with their corresponding shear moduli, Teter[6] discovered that hardness increases approximately with increasing shear moduli. Moreover, several other researchers[7,8] were able to find examples to support Teter's finding.

In fact, it is known that hardness measurements on brittle materials always accompany fracture:[9,10] creation and propagation of cracks. As a result, the resistance to fracture under shear, hydrostatic compression, as well as unloading, could be used to quantify the hardness. Next, we will try to identify physical parameters that play key roles in hardness measurements with the help of fracture mechanics and materials physics.

For materials without cracks, the theoretical stress to create a crack is given by the Orowan criterion[11]

$$\sigma_{\max} = (E\gamma_s/a_0)^{1/2}, \tag{1}$$

where γ_s is the surface energy of the material, E is Young's modulus, and a_0 is the inter-planar spacing in the unstressed state of the planes perpendicular to the tensile axis.

For materials with a crack under mode I loading (the loading is exerted normal to the cleavage plane), the theoretical stress intensity factor to propagate a crack is given by Griffith theory.[12] It states that the elastic driving force on an equilibrium crack is given by

$$\Gamma = (1-\nu)K_I^2/2G \tag{2}$$

where ν is Poisson's ratio, G shear modulus, and K_I stress intensity factor.

A crack propagates through breaking atomic bonds, and consequently new surfaces are created. The surface tension of the opening surfaces at the crack tip $2\gamma_s$ is the force to balance this elastic driving force. Therefore, the critical value of the stress intensity factor under mode I loading is given by

$$K_g = 2\sqrt{\gamma_s G/(1-\nu)}. \tag{3}$$

This equation is often called the Griffith relation. When the stress intensity factor of a crack reaches K_g, a crack propagates, which was observed in computer simulations.[13] K_g is the so-called theoretical fracture toughness,[14] which is applicable to the materials system without defects such as dislocations and other cracks. Since defects such as cracks and dislocations affect materials' response to the elastic driving force on the crack tip, an experimentally measured fracture toughness K_c can be considerably different from K_g in a system with defects.[14]

As surface energy is involved in creation and propagation of a crack, misfit energy is involved in creation and propagation of a dislocation. Misfit energy is the energy barrier encountered in the process of translating two rigid bodies along the slip plane, which is referred to as the γ surface.[15] The lattice resistance to dislocation motion is called Peierls stress. With the γ surface, Schoeck[16] calculated the Peierls stress based on the Peierls-Nabarro model.[17,18] It is generally believed that a major factor in determining the intrinsic ductile vs brittle behavior of materials is the ease of emission of dislocations from a crack tip. If a dislocation emission is sufficiently easy, then a crack will respond to an applied stress by such an emission and concomitant plastic deformation, rather than by crack extension. In 1974, Rice and Thomson[19] developed a semiquantitative criterion for intrinsic ductile vs brittle behavior based on a balance of forces on

the dislocation due to the applied stress and the image force. The disadvantage of this criterion is that there is a need to introduce an empirical dislocation core cutoff parameter. To overcome the disadvantage, Rice[20] used the maximum value of misfit energy so-called unstable stacking fault energy γ_{us} to characterize the resistance to dislocation nucleation from a crack. Under mode II loading (the loading is exerted in the cleavage plane, along the crack-propagation direction), the emission criterion is

$$K_{IIe} = \sqrt{2\gamma_{us}G/(1-\nu)}. \quad (4)$$

Zhou *et al.*[21] performed a series of atomistic calculations to establish criteria for dislocation emission from cracks and found that the new surface created at the blunted crack after dislocation emission must be added to the dislocation-emission theories based on misfit energy.

From the above analysis, it is evident that besides elastic parameters such as shear modulus and Poisson's ratio, other nonelastic materials parameters such as surface energy and unstable stacking fault energy are also needed for characterizing fracture, deformation, and hardness. For brittle materials where cracks rather than dislocations and twins are mostly involved in hardness measurement, we believe that theoretical fracture toughness could be an appropriate material parameter to characterize hardness. We are going to calculate theoretical fracture toughness for several brittle materials and to look at its relation with experimental hardness.

Since diamond, cubic boron nitride (*c*BN), boron suboxide (normally B_6O) are three known "superhard" materials [i.e., Vickers hardness (H_v) higher than 40 GPa], we chose them to investigate which parameters better characterize hardness. In addition, two more brittle materials, cubic SiC (3C-SiC) and Si, are also selected for our study. To avoid the complexity due to grain boundaries, we will focus on single-crystal behaviors of these five brittle materials.

Large grains of B_6O crystal have been recently synthesized[22–26] after 40 years since B_6O powder was made in laboratories.[27] He *et al.*[26] have succeeded to develop B_6O single crystals large enough to perform Vickers hardness measurements. Their measurements showed that the average hardness of crystalline B_6O is 45 GPa, close to the hardness of *c*BN, about 49 GPa.

However the parameters for determining the fracture toughness of B_6O are not available. In addition, there is no reported surface energy of *c*BN and 3C-SiC which is required in calculating their fracture toughness. Since density functional theory (DFT)[28] has been shown to be a reliable way of calculating material properties such as elastic constants[29] and material strength,[30] we will employ DFT total energy calculations to obtain shear modulus, bulk modulus, Young's modulus, Poisson's ratio, surface energies, and misfit energies of crystalline B_6O and the surface energy of crystalline *c*BN and 3C-SiC.

B_6O is of space group *R*-3*m* with a hexagonal unit cell of $a=b=5.3974$ Å and $c=12.3173$ Å.[24] In this paper *a*, *b*, and *c* are used to index the B_6O crystal planes and directions,[31] though a four Miller-Bravias index is also used. The positions of 6 oxygens and 32 borons can be obtained by using Wyckoff position operations on one oxygen position (0, 0, 0.6212), and two boron positions (0.1574, −0.1574, 0.6403), (0.2244, −0.2244, 0.7806).

TABLE I. Misfit energies of B_6O in the [100] direction. *a* is the lattice spacing of the unit cell along the [100] direction.

displacement(*a*)	1/8	2/8	3/8	4/8
$\gamma_{misfit}(J\,Å^{-2})$	2.24	5.12	4.62	4.97

After considering the requirements of the method accuracy and computational resources, we use either WIEN2K, a full-potential linearized augmented plane wave code,[32] or DFT++, a pseudopotential plane wave code.[33] WIEN2K will be used to calculate bulk modulus, Young's modulus, and Poisson's ratio involving high crystalline symmetry and DFT++ will be used to calculate surface energy, misfit energy, and shear modulus involving low crystalline symmetry.

In WIEN2K, the generalized gradient approximation (GGA) of PW2 type[34] is included to avoid any large inaccuracy in total energy calculations. The muffin-tin radius R_{MT} is 1.205 a.u. for oxygen and 1.575 a.u. for boron. The plan wave energy cutoff $R_{MT}K_{max}$ is 7, where R_{MT} is the smallest muffin-tin radius, e.g., 1.205 a.u. in the present calculation. To choose the number of *k* points for numerical integration at a given energetic precision, we performed a series of calculations with increasing the *k* points. It is found that 150 *k* points in the irreducible part of the Brillouin Zone can satisfy the energy convergence requirement.

In the calculation with DFT++, the Hamman type pseudopotentials of B, O, N, Si, and C ions are generated with the FHI98PP pseudopotential generation code,[35] and the energy cutoff is 24.0 Hartree. Although the cutoff is not large enough to guarantee convergence in total energy,[36] we find that this value can produce convergent results in the calculations of surface energies, misfit energies, and shear moduli where the difference in total energies rather than the absolute value of total energy is involved.

In Sec. II, we describe the calculations of surface and misfit energies. In Sec. III, bulk modulus, shear moduli G_{xy} and G_{xz}, Young's modulus, and Poisson's ratio of B_6O are calculated. In Sec. IV, we calculate the theoretical fracture toughness of diamond, *c*BN, B_6O, 3C-SiC, and Si and analyze the relationship between fracture toughness and hardness. We summarize in Sec. V.

II. MISFIT AND SURFACE ENERGIES

Misfit energy is defined as half the energy difference between one supercell consisting of two contiguous crystal unit cells sliding relative to each other and another supercell with two crystal unit cells without sliding. Misfit energies are calculated for the sliding displacements $a/8$, $2a/8$, $3a/8$, and $4a/8$ (Table I), where *a* is the lattice spacing of the B_6O hexagonal unit cell along the [100] direction. It is found that the so-called unstable stacking fault energy, the maximum value of the misfit energy, occurs at $2a/8$.

In order to calculate surface energies of a crystalline B_6O, an imaginary lattice, composed of infinite alternating slabs of real lattice and vacuum both of one lattice constant *c* thick, is

TABLE II. Surface energies (Jm^{-2}) of B_6O.

Surfaces	C	B_6O	*c*BN	3C—SiC	Si
(100)	5.7 (Ref. 37)	4.24	6.17	1.84	1.56 (Ref. 38)
(001)	5.7 (Ref. 37)	3.30	6.17	1.84	1.56 (Ref. 38)

used. The surface energy is defined as half the difference between energies in one unit cell of the imaginary lattice and one unit cell of the original lattice. Both (001) and (100) surface energies are calculated and listed in Table II. The significant difference between the two surface energies shows that a crystalline B_6O is highly anisotropic.

We also calculate the (001) surface energies of *c*BN and 3C-SiC. The surface energies just calculated and the reported surface energies for diamond and silicon are listed in Table II.

III. ELASTIC PROPERTIES

To calculate the Young's modulus, the B_6O unit cell is stretched along the $c(z)$ direction. The energetic gains of the stretched lattice as a function of the square of the stretching length along the z direction are fitted to a straight line (see Fig. 1). The restoring force is given by the slope of the fitted line. Thus we obtain the Young's modulus 507 GPa, which is about 7.8% larger than 470 GPa, the Young's modulus of a sintered compact B_6O with zero porosity.[39]

To obtain the shear modulus G_{xz}, shear strains ϵ_{xz} are applied to the unit cell to calculate the energy change as a function of ϵ_{xz}. The curve of calculated shear energy vs shear angle is fitted to a parabola as shown in Fig. 2.

The shear modulus is defined as $G=(F/S)/\theta$, where F is the force, S is the area of the base plane of the unit cell, and θ is the shear angle. The calculated shear modulus G_{xz} is 508 GPa, much larger than 204 GPa, the shear modulus of a polycrystalline B_6O.[6] Similarly, the shear modulus G_{xy} is obtained as 379 GPa. The considerable difference between G_{xy} and G_{xz} indicates that the B_6O is highly anisotropic as far as the shear modulus is concerned.

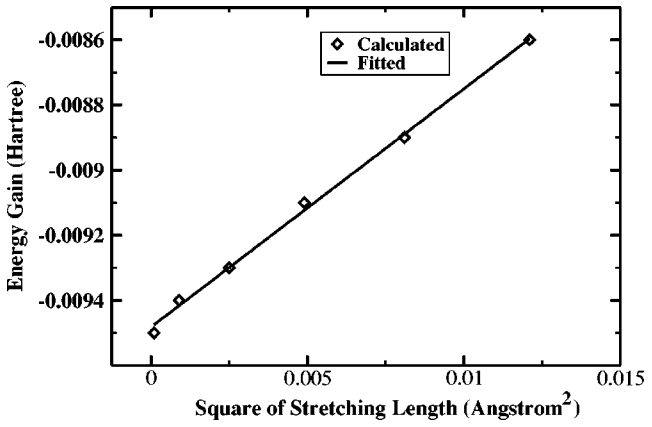

FIG. 1. The calculated energy gains as a function of the square of the stretching length of a B_6O unit cell. Diamonds are the calculated values, while the line is the linear fit to the energy gains.

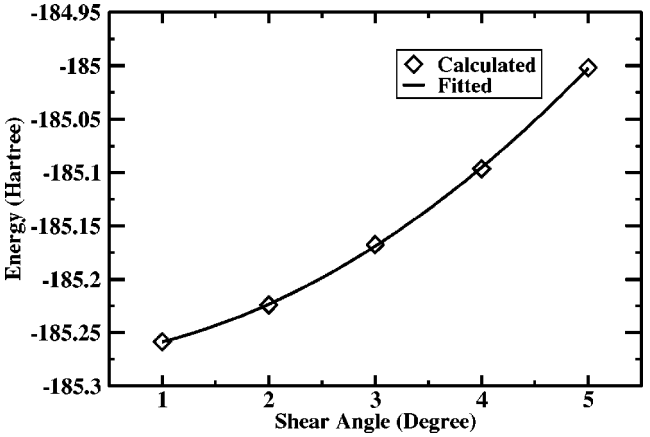

FIG. 2. Total energy changes as a function of the shear angle for a distorted B_6O unit cell under a shear strain ϵ_{xz}. Diamond denotes the calculated value, while the line is the parabola fit to those points.

In the calculation of the bulk modulus, we simulate the hydrodynamic strain by fixing the ratio of c/a. By fitting the points of calculated total energies vs volumes to Murnaghan's equation of state,[44] we obtain the bulk modulus 238 GPa.

A number of calculated bulk moduli have been reported. With a plane-wave pseudopotential DFT code, Lee *et al.*[45] obtained the bulk modulus 228 GPa. Using VASP, also a plane-wave pseudopotential DFT code, Xie *et al.*[46] obtained the bulk modulus 220 GPa. Our calculated value 238 GPa is higher than those reported values. It is likely due to the fact that we use fixed ratio of c/a which leads to the upper limit of bulk modulus as pointed out by Mehl *et al.*[47]

Because the experimentally measured value of the bulk modulus of a sintered B_6O is 222 GPa,[48] and a single crystal is expected to have a larger bulk modulus than that of a sintered one, we think that the value, 228 GPa, obtained by Lee *et al.*,[45] is a good representation of the bulk modulus of a single crystal. Therefore we will use it to calculate the Poisson's ratio in the following paragraph.

To calculate the Possion's ratio, a unit cell is stretched along the *c* direction, and contracted in the *a* and *b* directions. In our calculation, we stretch the *c* axis of the unit cell by 0.2155 Å. After adjusting the lengths of *a* and *b* axes of the unit cell simultaneously, we calculate total energies. Then the change of the *a* and *b* axes at the minimum-energy configuration is identified as 0.0141 Å and consequently the contraction strain, 0.0026 is obtained. Finally the Poisson's ratio is found to be 0.14. Meanwhile, under the isotropic assumption, the Poisson's ratio is given by $\nu=(3B-E)/(6B)$.[49] With our calculated bulk and Young's modulus, we obtain the value of Poisson's ratio 0.13 which is very close to 0.14 calculated directly with DFT.

To investigate the relationship among hardness and elastic parameters, we list bulk modulus, shear modulus, Young's modulus, and Poisson's ratio in Table III. In addition, we list in Table III the averaged shear modulus with the definition of $G_{ave}=0.5[C_{44}+0.5(C_{11}-C_{12})]$.

TABLE III. Elastic properties: bulk modulus B, average shear modulus $G_{ave}=0.5[C_{44}+0.5(C_{11}-C_{12})]$, shear modulus G of a defined surface, Young's modulus E, and Poisson's ratio ν.

	Direction	C (Ref. 40)	*c*BN (Ref. 41)	B_6O	3C—SiC (Ref. 42)	Si (Ref. 43)
B(GPa)		442	400	228	223	98
G_{ave}(GPa)		528	398	443	217	66
G(001)(GPa)		478	315	508	147	51
G(100)(GPa)				379		
E(GPa)	[001]	1050	748	507	362	130
ν	[001]	0.10	0.18	0.14	0.23	0.28

IV. FRACTURE TOUGHNESS AND HARDNESS

With newly calculated surface energies, shear moduli, and Poisson's ratio of B_6O, we calculate its theoretical fracture stress σ_{max} with Eq. (1) and theoretical fracture toughness K_g with Eq. (3). σ_{max} is about 35 $GPam^{-1}$ for the (001) fracture plane. K_g is about 2.7 $MPam^{1/2}$ for the (001) as well as for the (100) fracture plane.

To investigate the relationship among hardness, shear modulus, theoretical fracture stress, and fracture toughness in brittle materials, we also calculated K_g and σ_{max} for diamond, *c*BN, 3C-SiC, and Si. Their values along with B_6O's are listed in Table IV.

For the five materials we are studying (Si, 3C-SiC, B_6O, 3C-SiC, *c*BN, and diamond), we plot K_g (see Table IV) for the (001) fracture plane and G_{ave} (see Table III) against the experimental value of Vickers hardness (see Table IV) in Figs. 3 and 4, respectively. The Vickers hardness H_v is chosen as the vertical axis in both figures. The ascending trend of hardness for Si, 3C-SiC, B_6O, *c*BN, and diamond is correctly correlated with the theoretical fracture toughness (see Fig. 3) but not with the average shear modulus (see Fig. 4). That is, the correlation between K_g and H_v is better than that between G_{ave} and H_v. Thus our conjecture that theoretical fracture toughness can be a better material parameter to characterize hardness of brittle materials is supported by data.

The experimental value of fracture toughness for a single crystal K_c is 5 $MPam^{1/2}$ for diamond,[50] 2.8 for *c*BN,[51] 4.5 for B_6O,[26] 0.78 for 3C-SiC,[52] and 0.75 for silicon.[52] Experimentally measured fracture toughness can be quite different from the theoretical fracture toughness K_g due to loading conditions, orientations of cracks, preexisting defects, etc., in experimental specimens. In particular, the values of fracture toughness derived from indentation experiments could scatter considerably due to uncertainty of measured crack lengths.[53] The experimental value of hardness is not unique either. For example, Zhao *et al.*[54] reported that the hardness appears to increase with the decrease in load in BC_2N and *c*BN samples. Lately Zhao *et al.*[55] have further investigated this issue in hard and brittle materials and suggested that the hardness and fracture toughness should be taken after the visible propagation of macrocracks, i.e., pass the bend in the curve of H_v vs loading force, when hardness approaches its asymptotic value. (The most recent measurement on single-crystal Moissantite-6H SiC clearly shows that the hardness approaches its asymptotic value as the loading goes beyond 100N.[53]) They believe that this behavior of hardness as a function of loading force is likely behind a wide disparity in the reported experimental values of hardness and fracture toughness.

V. DISCUSSION AND SUMMARY

By using DFT total energy calculations implemented with pseudopotential plane waves as well as full potential linearized augmented plane waves, we obtained bulk, Young's and shear elastic moduli, Poisson's ratio, surface energies, and unstable stacking fault energy of crystalline B_6O. In addition, we calculated the (001) surface energies of 3C-SiC and *c*BN. The calculated values of elastic moduli agree reasonably well with experimental ones of polycrystalline B_6O. With those newly calculated and reported materials parameters, we were able to obtain theoretical fracture toughness and theoretical fracture stress.

Theoretical fracture stress characterizes the barrier for creating a crack in a crystal without defects, while theoretical fracture toughness describes the barrier for an existing crack to propagate. As shown in Eqs. (1) and (3), both parameters are proportional to $(\gamma_s G)^{1/2}$. Because of the narrow range of Poisson's ratio, its role in determining fracture toughness is much smaller than shear modulus and surface energy. Since

TABLE IV. Theoretical fracture toughness K_g, theoretical fracture stress σ_{max}, and Vickers hardness H_v.

	C	*c*BN	B_6O	B_6O	3C—SiC	Si
surfaces	(001)	(001)	(001)	(100)	(001)	(001)
K_g($MPam^{1/2}$)	3.4	2.9	2.7	2.7	1.0	0.6
σ_{max}($GPam^{-1}$)	168	95	35		41	19
H_v(GPa)	90 (Ref. 26)	48 (Ref. 26)	45 (Ref. 26)	45 (Ref. 26)	28 (Ref. 6)	10 (Ref. 6)

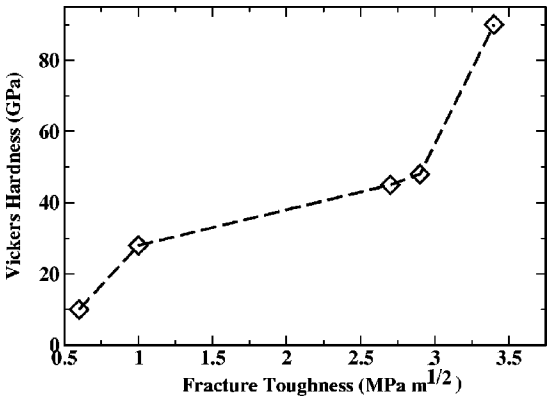

FIG. 3. Vickers hardness as a function of calculated theoretical fracture toughness. The Vickers hardness increases in the order of Si, 3C-SiC, B_6O, *c*BN, and diamond. Diamond denotes the calculated value and the dashed line is for visualization.

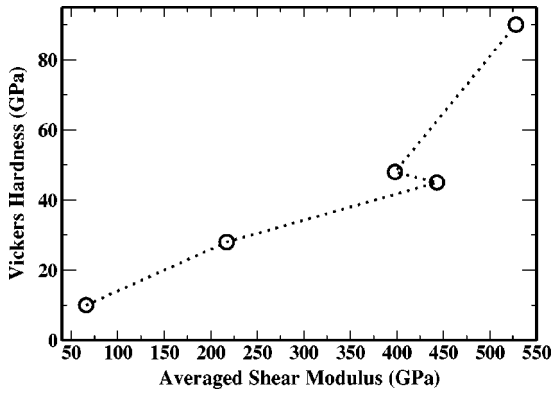

FIG. 4. Vickers hardness as a function of averaged shear modulus. As in Fig. 3, the Vickers hardness increases in the order of Si, 3C-SiC, B_6O, *c*BN, and diamond. Circle denotes the calculated value and the dotted line is for visualization.

in a brittle crystal, creation and propagation of cracks, rather than dislocations and twins, are mostly involved in the experimental measurement of hardness, a physical parameter, surface energy, to describe creation of new surfaces due to cracks, a nonelastic process, has to be included in characterizing hardness. Therefore, we believe that the theoretical fracture toughness which is proportional to $(\gamma_s G)^{1/2}$ should be used for characterizing the hardness of brittle materials rather than elastic parameters alone, such as bulk or shear modulus. The analysis of diamond, *c*BN, B_6O, 3C-SiC, and Si supports such an argument (see Table IV, Figs. 3 and 4). In his empirical relationship between shear modulus and hardness, Teter[6] seems to use an averaged shear modulus to characterize Vickers hardness, which is defined as the average of the tetragonal and rhombohedral shear moduli, $(C_{11}-C_{12})/2$ and C_{44}, respectively.[8] Other similar definitions such as the Voigt averaged shear modulus, $G=(3C_{44}+C_{11}-C_{12})/5$, may serve the same purpose.[7] The average of our calculated G_{xy} $[=(C_{11}-C_{12})/2]$ and G_{xz} $(=C_{44})$ of B_6O, 443 GPa is larger than the average shear modulus of *c*BN, 398 GPa. If we use Teter's empirical relationship between average shear modulus and hardness, the H_v of B_6O is likely larger than that of *c*BN. But the experimental value of H_v of B_6O is about 45 GPa, smaller than that of *c*BN, 49 GPa. However K_g gives a correct order. Apparently, a systematic investigation of relationship between hardness and theoretical fracture toughness in a wider range of brittle materials would be very helpful for further validating our conjecture. Becuase of the role of surface energy in the theoretical fracture toughness, surface specified hardness should have better correlation with fracture toughness.

It is interesting to note that Gao *et al.*[56] have recently proposed a semiempirical method for evaluating hardness of covalent crystals based on electronic structure. They found that bond density or electronic density, bond length, and degree of covalent bonding are three determinative factors for the hardness of a polar covalent crystal. Their method is based on the fact that atomic bonds are broken in the process of indentation, which certainly cannot be fully characterized with elastic parameters alone, such as shear modulus. In our study, surface energy is used to characterize the breaking event of atomic bonds.

Our study is established on the physics and mechanics of fracture that basically deal with the energetic balance between elastic driving force at a crack tip and material response. Therefore, it covers both elastic and nonelastic aspects of indentation creation in hardness measurements. The key quantity is found to be $(\gamma_s G)^{1/2}$. Because surface energy and shear modulus are both theoretically calculable and experimentally measurable, we believe that characterizing hardness in hard and brittle materials in terms of $(\gamma_s G)^{1/2}$ provides a direct guidance to materials synthesis.

ACKNOWLEDGMENTS

This work was partly performed under the auspices of the U.S. Department of Energy (DOE) under Contract No. W-7405-ENG-36 with the University of California.

*Email address: szhou@pegasus.me.jhu.edu

[1] L. T. Small, *Hardness, Theory and Practice* (Service Diamond Tool Co., Ferndale, Michigan, 1960).
[2] W. Zhang and G. Subhash, Int. J. Solids Struct. **38**, 5893 (2001).
[3] R. J. Goble and S. D. Scott, Can. Mineral. **23**, 273 (1985).
[4] A. Y. Liu and M. L. Cohen, Science **245**, 841 (1989).
[5] J. M. Leger, J. Haines, M. Schmidt, J. P. Petitet, A. S. Pereira, and J. A. H. Dajornada, Nature (London) **383**, 401 (1996).
[6] D. M. Teter, MRS Bull. **23**, 22 (1998).
[7] J. M. Leger, P. Djemia, F. Ganot, J. Haines, A. S. Pereira, and J. A. H. da Jornada, Appl. Phys. Lett. **79**, 2169 (2001).
[8] C. Kocer, N. Hirosaki, and S. Ogata, Phys. Rev. B **67**, 035210 (2003).
[9] G. R. Anstis, P. Chantikul, B. R. Lawn, and D. B. Marshall, J.

Am. Ceram. Soc. **64**, 533 (1981).
[10] B. R. Lawn and D. M. Marshall, J. Am. Ceram. Soc. **62**, 347 (1979).
[11] A. Kelly, *Strong Solids* (Clarendon, Oxford, 1973).
[12] A. A. Griffith, Philos. Trans. R. Soc. London, Ser. A **221**, 163 (1920).
[13] S. J. Zhou, A. E. Carlsson, and R. Thomson, Phys. Rev. B **47**, 7710 (1993).
[14] R. Thomson, Solid State Phys. **39**, 1 (1986).
[15] V. Vitek, Philos. Mag. **18**, 773 (1968).
[16] G. Schoeck, Philos. Mag. A **63**, 111 (1991).
[17] R. R. Peierls, Proc. Phys. Soc. London **52**, 34 (1940).
[18] F. R. N. Nabarro, Proc. Phys. Soc. London **59**, 256 (1947).
[19] J. R. Rice and R. Thomson, Philos. Mag. **29**, 73 (1974).
[20] J. R. Rice, J. Mech. Phys. Solids **40**, 239 (1992).
[21] S. J. Zhou, A. E. Carlsson, and R. Thomson, Phys. Rev. Lett. **72**, 852 (1994).
[22] H. Hubert, B. Devouard, L. A. J. Garvie, M. O'Keeffe, P. R. Buseck, W. T. Petuskey, and P. F. McMillan, Nature (London) **391**, 376 (1998).
[23] H. Hubert, L. A. J. Garvie, B. Devouard, P. R. Buseck, W. T. Petuskey, and P. F. McMillan, Chem. Mater. **10**, 1530 (1998).
[24] D. W. He, M. Akaishi, B. L. Scott, and Y. S. Zhao, J. Mater. Res. **17**, 284 (2002).
[25] S. Yu, G. Wang, S. Yin, Y. Zhang, and Z. Liu, Phys. Lett. A **268**, 442 (2000).
[26] D. W. He, Y. S. Zhao, L. Daemen, J. Qian, T. D. Shen, and T. W. Zerda Appl. Phys. Lett. **81** 643 (2002).
[27] H. F. Rizzo, W. C. Simmons, and H. O. Bielstein, J. Electrochem. Soc. **109**, 1079 (1962).
[28] M. C. Payne, M. P. Teter, D. C. Allan, T. A. Arias, and J.D. Joannopoulos, Rev. Mod. Phys. **64**, 1045 (1992).
[29] L. Fast, J. M. Wills, B. Johansson, and O. Eriksson, Phys. Rev. B **51**, 17 431 (1995).
[30] R. H. Telling, C. J. Pickard, M. C. Payne, and J. E. Field, Phys. Rev. Lett. **84**, 5160 (2000).
[31] http://www. uwgb.edu/dutchs/symmetry/millerdx.htm
[32] P. Blaha, K. Schwarz, G. K. H. Madsen, D. Kvasnicka, and J. Luitz, *WIEN2K, An Augmented Plane Wave+Local Orbitals Program for Calculating Crystal Properties* (Technische Universitat Wien, Austria, 2001).
[33] S. Ismail-Beigi and T.A. Arias, Comput. Phys. Commun. **128**, 1 (2000).
[34] J. P. Perdew and Y. Wang, Phys. Rev. B **45**, 13 244 (1992).
[35] M. Fuchs and M. Scheffler, Comput. Phys. Commun. **119**, 67 (1999).
[36] S. Lee, S. W. Kim, D. M. Bylander, and L. Kleinman, Phys. Rev. B **44**, 3550 (1991).
[37] J. Furthmuller, J. Hafner, and G. Kresse, Phys. Rev. B **53**, 7334 (1996).
[38] D. M. Bird, L. J. Clarke, R. D. King-Smith, M.C. Payne, I. Stich, and A. P. Sutton, Phys. Rev. Lett. **69**, 3785 (1992).
[39] D. R. Petrak, R. Ruh, and G. R. Atkins, Am. Ceram. Soc. Bull. **83**, 569 (1974).
[40] H. J. McSkimin and P. Andreatch, Jr., J. Appl. Phys. **43**, 2944 (1972).
[41] M. Grimsditch and E.S. Zouboulis, J. Appl. Phys. **76**, 832 (1994).
[42] W.R.L. Lambrecht, B. Segall, M. Methfessel, and M. van Schilfgaarde, Phys. Rev. B **44**, 3685 (1991).
[43] H. J. McSkimin, J. Appl. Phys. **24**, 988 (1953).
[44] F. D. Murnaghan, Proc. Natl. Acad. Sci. U.S.A. **3**, 244 (1944).
[45] S. Lee, D.M. Bylander, and L. Kleinman, Phys. Rev. B **45**, 3245 (1992).
[46] J. J. Xie, S. P. Chen, J. Wills, and Y. S. Zhao (unpublished).
[47] M. J. Mehl, J. E. Osburn, D. A. Papaconstantopoulos, and B. M. Klein, Phys. Rev. B **41**, 10 311 (1990).
[48] M. C. Tushishvili, C. V. Tsagareishvili, and D. S. Tsagareishvili, J. Hard Mater. **3**, 225 (1992).
[49] M. Levy, in *Handbook of Elastic Properties of Solids Liquids and Gases*, edited by M. Levy, H. Bass, and R. Stern (Academic Press, London, 2001).
[50] N. V. Novikov and S. N. Dib, J. Hard Mater. **2**, 3 (1991).
[51] C. A. Brookes, Inst. Phys. Conf. Ser. **75**, 207 (1986).
[52] X. Li and B. Bhushan, Thin Solid Films **340**, 210 (1999).
[53] J. Qian and Y. S. Zhao, Diamond Related Mater. (to be published).
[54] Y. Zhao, D. W. He, L. L. Daemen, J. Huang, T. D. Shen, R. B. Schwarz, Y. Zhu, D. L. Bish, J. Zhang, G. Shen, J. Qian, and T. W. Zerda, J. Mater. Res. **17**, 3139 (2002).
[55] Y. Zhao, J. Qian, L. L. Daemen, C. Pantea, J. Zhang, G. A. Voronin, and T. W. Zerda, Appl. Phys. Lett. **84**, 1356 (2004).
[56] F. Gao, J. He, E. Wu, S. Liu, D. Yu, D. Li, S. Zhang, and Y. Tian, Phys. Rev. Lett. **91**, 015502 (2003).